Earth Science Informatics (2024) 17:2775–2789
https://doi.org/10.1007/s12145-024-01311-9

SOFTWARE

RadonPotential: An interactive web application for radon potential prediction under different climates and soil textures

Juan Jose Galiana-Merino[1,2] · Sara Gil-Oncina[3] · Javier Valdes-Abellan[4] · Juan Luis Soler-Llorens[3] · David Benavente[3]

Received: 29 October 2023 / Accepted: 10 April 2024 / Published online: 19 April 2024

Abstract

The presence of radon in soil poses a significant health risk when it enters and concentrates indoors. The primary health problem associated with radon exposure is lung cancer, but it can also contribute to other respiratory issues. Estimating radon potential is a challenging task caused by the interaction of various environmental, geological, and variability factors. Although efforts are ongoing to improve radon potential assessment methodologies, there is a lack of software tools that estimate and model radon potential in different scenarios. The paper aims to develop a novel web-based software tool, RadonPotential, that predicts Geogenic Radon Potential by considering variations in climate and soil textures.

The program runs using a constant radon concentration or estimates its concentration from the radium activity. RadonPotential calculates the transport of radon through a soil profile based on water content and soil texture. It also determines the dynamics of soil water content in different climates, incorporating long-term weather data under various climatic scenarios and local weather time series. The web-based format of the program increases its dissemination, usage, and manageability among a larger user base compared to an installable computer program. The program aims to provide a simplified and effective characterization of radon potential levels accessible to a wide range of scientists, technical experts and policymakers in developing strategies not only for radon measurement and mitigation buildings but also for developing more reliable large-scale radon potential maps.

Keywords Geogenic radon potential · Indoor radon · HYDRUS-1D · MATLAB Web Server

Introduction

Radon, also known as Rn, is a naturally occurring radioactive gas found in nearly all soils and rocks on Earth's surface. In general, radon studies focus on the ^{222}Rn isotope because it has a longer half-life (3.825 days) compared to the other isotopes (^{220}Rn and ^{219}Rn). It represents the primary origin of ionizing radiation throughout naturally occurring substances (World Health Organization 2009). Radon originates from the radium decay, specifically ^{226}Ra, which is part of the decay chain of ^{238}U. Radon has been widely used in diverse applications in the field of geoscience, highlighting its potential use as an indicator of earthquakes and tectonic stress, particularly in volcanic regions as well as a valuable

Communicated by H. Babaie

✉ Juan Jose Galiana-Merino
jj.galiana@ua.es

Sara Gil-Oncina
sara.gil@ua.es

Javier Valdes-Abellan
javier.valdes@ua.es

Juan Luis Soler-Llorens
jl.soler@ua.es

David Benavente
david.benavente@ua.es

[1] Department of Physics, Systems Engineering and Signal Theory, University of Alicante, 03690 Alicante, Spain

[2] University Institute of Physics Applied to Sciences and Technologies, University of Alicante, 03690 Alicante, Spain

[3] Department of Earth and Environmental Sciences, University of Alicante, 03690 Alicante, Spain

[4] Department of Civil Engineering, University of Alicante, 03690 Alicante, Spain

tracer in marine and hydrological environments (Tareen et al. 2019; Morales-Simfors et al. 2020; Vital et al. 2022; Galiana-Merino et al. 2022).

In confined spaces such as residence basements, workplaces, underground mines, and caves, radon can be accumulated to elevated levels, presenting a significant health hazard (Elío et al. 2018). Consequently, the World Health Organization (WHO) has identified radon as the second leading cause of lung cancer, following smoking, in numerous developed nations (World Health Organization 2009).

In many cases, the primary source of indoor radon can be attributed to the geological composition beneath and surrounding buildings. The concept of Geogenic Radon Potential (GRP) is defined to assess the radon risk and posits that the main contributor to indoor radon concentration is radon gas emanating from the soil. GRP can be considered an optimal Rn hazard indicator as it conceptualizes "what Earth deliveries in terms of radon" from the geogenic sources (e.g., radionuclides in soils and rocks, fractures and faults) to the atmosphere (Gruber et al. 2013; Bossew et al. 2020). Uranium and radium-rich soils and rocks serve as a reservoir for radon gas, and its movement towards the surface can be facilitated by permeable materials (Appleton 2007). A well-established method for calculating the GRP of a particular zone was introduced by Neznal et al. (2004), which contemplates the permeability of the soil and the concentration of the soil radon gas by Eq. (1):

$$GRP = \frac{CRn}{pk_g - 10} \tag{1}$$

where CRn is the equilibrium radon activity concentration in soil gas, expressed as kBq/m^3; and k_g is the soil permeability, which is defined as $pk_g = -\log(k_g)$. Low pk_g values imply permeable soils. There is no consensus about GRP units. Most authors consider GRP as a dimensionless value, while others express GRP in radon activity concentration (kBq/m^3). In this web application, GRP does not consider units to avoid confusion. GRP can be classified as low ($GRP < 10$), medium ($10 \leq GRP < 35$) and high ($GRP \geq 35$) risk, according to the Neznal et al. (2004) classification. Consequently, an elevated GRP value implies a higher probability of indoor radon infiltration due to geological factors.

Estimation of the GRP value in a particular area involves performing in-situ measurements of gas permeability and Rn concentration in the soil, conventionally measured at 1 m depth, as recommended by the International Organization for Standardization for measurements of radioactivity in the environment (ISO Standard No. 11665–11:2016) (https://www.iso.org/standard/63787.html). However, in most cases, the onsite measurement of soil permeability is difficult and time-consuming. As we will describe in Sect. 2.4, soil permeability and the theoretical calculation of ^{222}Rn concentration from ^{226}Ra activity are sensitive to the soil water content and the soil texture, which limits the estimation of the GRP. Additionally, the use of this method for the evaluation of the GRP is based on a single measurement, while radon-related health risks arise from prolonged exposure to specific dosage levels.

In general, the determination of the potential radon is carried out through onsite surveys, following the methodology developed in the Czech Republic, which combines measurements of radon concentration and soil permeability (Neznal, 2004). Large-scale mapping of GRP serves as a tool for radon risk management for homes at both regional and national levels, as well as internationally (Farias et al. 2016; Petermann et al 2021). At the European level, the European Atlas of Natural Radiation includes geogenic information about soils, such as geological units, uranium and radium geochemical maps, soil clay fraction, and other relevant data (Cinelli et al. 2019). For example, the European map of soil uranium concentration displays the estimated uranium concentration in 10 km × 10 km cells. This map was created using approximately 5000 soil sample data from two European databases: (i) the Geochemical Atlas of Europe, developed by the Forum of European Geological Surveys (Salminen et al., 2005), and (ii) the geochemical map of agricultural and grazing soils in Europe (GEMAS) (Demetriades et al. 2021). The methodologies for estimating indoor radon concentration rely on interpolation techniques (statistical and/or geostatistical) based on uranium concentration, permeability, and other factors. Elío et al. 2019) used 1.2 million radon samples measured inside homes to create the European indoor radon map.

However, the existing methodologies fail to incorporate soil water content and its impact on radon emanation and soil gas permeability, despite its significance in gas movement through porous media (Benavente et al. 2019). Soil water content in a particular region is closely linked to the soil texture and climatic factors, such as precipitation and temperature patterns. These variables must be taken into consideration when examining radon transport in soils and assessing radon potential. Furthermore, variations in soil moisture content across the four seasons must be considered in the GRP assessment, as soil moisture and soil gas permeability can undergo significant changes throughout the year (Gil-Oncina et al. 2022).

This paper aims to develop a novel procedure for predicting radon potential, considering variations in climate and soil textures. Firstly, we describe the equations that define the radon concentration and transport through a soil profile in terms of water moisture and soil texture. Secondly, we determine the dynamics of soil water content in different climates, incorporating long-term weather data under various climatic scenarios and local weather time series. Finally, we assess the variations in Geogenic Radon

Potential risk resulting from the temporal variability of climatic conditions or local weather patterns. All this theoretical development has been implemented under a novel software, called RadonPotential, which has been designed as a web-based application that can be run from any web browser. This software allows a simplified and effective characterization of the radon potential level, accessible to a wide range of scientists, technical professionals and policymakers.

The rest of the paper is organized as follows. In Sec.2 we introduce the theoretical background of soil water moisture dynamics, radon permeability and meteorological influence. In Sec. 3, the developed software is described in detail. After that, some case studies are introduced in Sec. 4, followed by the main conclusions in Sec. 5.

Methods

Soil texture and hydraulic properties

The USDA (United States Department of Agriculture) texture classification is established by combinations of different percentages of sand, silt and clay (% SSC) in a ternary diagram (United States Department of Agriculture 1987). The soil unsaturated hydraulic conductivity is based on the van Genuchten–Mualem model constitutive relationships (vGN) (Mualem 1976; van Genuchten 1980). This model relates the saturated hydraulic conductivity Ks [LT-1]; the saturated water content, θs [L^3 L^{-3}]; the residual water content θr [L^3 L^{-3}]; and two empirical parameters that define the shape of the hydraulic functions, α [L^{-1}] and n [-]. α and n coefficients are critical to shaping soil hydraulic functions in the unsaturated systems. α is associated with air-entry value whereas pore size distribution is linked to n. These soil hydraulic parameters for unsaturated soils are estimated using the Rosetta 3 pedotransfer function, PTF, (Zhang and Schaap 2017) according to the methodology described by Benavente et al. (2019). The Rosetta prediction is based on the % SSC and the soil bulk density, ρ_b (g cm^{-3}).

In the RadonPotential application, soil properties are defined using basic parameters (% SSC and the soil bulk density). However, soil structure and, in general, pedological properties, can locally modify radon emanation and movement. This depends on factors such as the parent material, the chemistry and structure of minerals (e.g., the presence of clay minerals), biological activity (e.g., organic matter, root growths or macropores due to animal burrow holes, etc.), and environmental conditions (such as the presence of shrinking or swelling clays, or freezing and thawing) (Cinelli et al. 2019).

Soil water content dynamics

Soil water content, θ, and soil water flow have been simulated using the software HYDRUS-1D (Šimůnek et al. 2009), which works out numerically the Richards equation (Richards 1931) for variable-saturated soil water conditions according to Eq. (2):

$$\frac{\partial \theta}{\partial t} = \frac{\partial}{\partial z}\left(K(h) \cdot \left(\frac{\partial h}{\partial z} + 1\right)\right) - S(h) \quad (2)$$

where $K(h)$ is the soil unsaturated hydraulic conductivity [$L\ T^{-1}$]; $S(h)$ is the sink term that denotes water uptake by plants [$L^3\ L^{-3}\ T^{-1}$]; z is the vertical coordinate [L]; and t is time [T].

A vertical soil profile of 200 cm deep has been established for all simulations and soil-climate combinations. The simulated soil profile has been discretized using 210 nodes. The distance between numerical nodes ranges from 1 mm at the top-soil surface to 1 cm at 10 cm depth. From 10 cm downward, the distance of 1 cm between numerical nodes remains constant. Simulated soil water content and soil pressure have been selected for 20, 50, 80 and 100 cm, although the calculation of GRP has been only based on predictions at 100 cm because it is the reference depth for radon potential studies. 100 cm depth is chosen to avoid dilution of the soil radon sample with atmospheric air, as recommends the International Organization for Standardization for measurements of radioactivity in the environment (ISO Standard No. 11665–11:2016) (https://www.iso.org/standard/63787.html).

Atmospheric conditions and free drainage options have been selected in the upper and bottom boundaries, respectively. Regarding the atmospheric data required for the upper boundary, two alternatives may be considered: user-entry information or user climate selection. In the case of the latest option, the code automatically creates a temporal series of precipitation and potential ET_0 based on an adaptation of the Hargreaves equation (Williams et al. 2008; Martínez et al. 2014). The initial condition has been established as a constant soil pressure head. The consequences of this subjective decision have been counteracted by the introduction of a warm-up period, as it will be shown in Sect. 2.5.

Gas permeability in unsaturated soils

Increasing water content in porous materials leads to a decrease in gas permeability, which influences radon potential. The presence of moisture in these materials decreases both the size of the pores and the effective porosity, and at the same time increases the tortuosity

(Benavente and Pla 2018). The estimation of unsaturated gas permeability, $k_g(S_w)$, follows the approach suggested by Benavente et al. (2019) and it is formulated as Eq. (3):

$$k_g(S_W) = k_g\left(1 - S_W^{\tau}\right) \cdot \left[1 - \left(1 - \left(1 - S_W^{m^{-1}}\right)^{m}\right)^{2}\right] \quad (3)$$

where the water saturation, S_w, is defined by Eq. (4):

$$S_W = \frac{\theta(h) - \theta_r}{\theta_s - \theta_r} \quad (4)$$

where k_g is the variable-saturated gas permeability; h is the soil pressure head [L]; θ ($cm^3\ cm^{-3}$) is the measured volumetric water content; α [L^{-1}] and n [-] are the vGN parameters; and τ [-] is the tortuosity value (commonly $\tau = 0.5$) (Mualem 1976). m [-] is calculated as $m = 1\text{-}n^{-1}$.

Using % SSC and the bulk density of soil as input values, Rosetta PTF calculates the vGN parameters and the saturated hydraulic conductivity, Ks (cm day^{-1}). In the case of considering pure water at 20ºC, the saturated hydraulic conductivity can be expressed as Ks (m^2) = $1.18 \cdot 10^{-14}$ ·Ks (cm day^{-1}) and considered equal to k_g. After that, $k_g(S_w)$ is then computed in terms of the effective water saturation, calculated from HYDRUS-1D (Eq. (4)) at different soil depths for any soil-climate combination. Normally, k_g is expressed logarithmically as $pk_g = -\log(k_g)$, so this will be the term used in this work.

Theoretical ^{222}Rn concentration from ^{226}Ra activity

The estimation of radon potential requires the measurement of ^{222}Rn concentration in soils. However, obtaining accurate measurements can be challenging, depending on factors such as the type and availability of equipment, depth of the soil profile, and water content. Additionally, ^{222}Rn concentration is known to fluctuate due to climatic conditions (Victor et al. 2019; Pla et al. 2023; Alegría et al. 2023), requiring the application of reliable estimation methods. ^{222}Rn can be estimated from ^{226}Ra activity because it is a decay product of ^{226}Ra generated in the radioactive decay series of ^{238}U. Thus, ^{222}Rn is produced in the soil matrix by the existence of ^{226}Ra. It has to move back into the pore space (Elío et al. 2019), and therefore its concentration in soil gas is dependent on both ^{226}Ra concentration and soil properties, mainly soil density, effective porosity, and an emanation coefficient. Thus, the theoretical ^{222}Rn concentration in soil gas due to ^{226}Ra can be obtained through Eq. (5) (e.g., Akerblom 1993; Voltaggio et al. 2006; Giustini et al. 2019):

$$CRn = CRa \cdot \epsilon \cdot \rho_b \quad (5)$$

where CRa (Bg kg^{-1}) is the ^{226}Ra activity, ε (-) is the emanation coefficient, and ρ_b (g cm^{-3}) is the bulk density. The emanation coefficient of ^{222}Rn in soil can be obtained by Eq. (6) (Zhuo et al. 2006, 2008):

$$\varepsilon = \varepsilon_0 \cdot \left[1 + a\left(1 - \exp\left(-b \cdot S_W\right)\right)\right] \cdot [1 + c \cdot T] \quad (6)$$

where ε_0 is the ^{222}Rn emanation coefficient at 25 ºC for dry soil; S_w is the water saturation (Eq. (4)); T (ºC) is the soil temperature; and a, b, and c are three fitted parameters, which depend on the characteristics of the soil. In Table 1, the values of the fitted parameters for clay, silt and sand are shown. In addition, in Table 2, the percentages of clay, silt and sand for different soil textures are also presented.

Combining the values of these coefficients (Table 1) with the percentages of clay, silt and sand (e.g., Table 2), the fitted parameters and the ^{222}Rn emanation coefficient can be estimated for any type of soil texture as a weighted sum, that is (% Sand)·$\varepsilon_{0,sand}$ + (% Silt)·$\varepsilon_{0,silt}$ + (% Clay)·$\varepsilon_{0,clay}$. Thus, for example, the ^{222}Rn emanation coefficient for a loamy sand soil can be calculated as $\varepsilon_{0,soil} = (83/100)\cdot\varepsilon_{0,sand} + (12/100)\cdot\varepsilon_{0,silt} + (5/100)\cdot\varepsilon_{0,clay}$.

Therefore, the estimation of the theoretical ^{222}Rn concentration requests of ^{226}Ra activity, soil texture, water content and temperature.

Table 1 Fitted parameters and ^{222}Rn emanation coefficient for clay, silt and sand (Zhuo et al. 2008)

Coefficient	Clay	Silt	Sand
ε_0	0.10	0.14	0.18
a	1.85	1.73	1.53
b	18.8	20.5	21.8
c	0.012	0.01	0.011

Table 2 Percentage of sand, silt and clay (% SSC) according to the USDA soil texture classification (Zhuo et al. 2008)

Texture	% Sand	% Silt	% Clay
Clay	5	5	90
Clay Loam	33	34	33
Loam	42	41	17
Loamy Sand	83	12	5
Sand	90	5	5
Sandy Clay	52	7	41
Sandy Clay Loam	60	12	28
Sandy Loam	65	25	10
Silt	5	90	5
Silty Clay	7	47	46
Silty Clay Loam	10	55	35
Silty Loam	22	68	10

In this way we see that the GRP can be obtained either using a constant value of radon concentration in soil, measured experimentally on site, or using a theoretical estimate, based on other parameters, as explained in this section.

Meteorological time series

The influence of climate on GRP can be evaluated considering two types of approximations: long-term weather scenarios and shorter meteorological time series.

Long-term weather scenarios are defined according to the Köppen climate classification (Köppen 1936), which has had constant updates. For example, Beck et al. (2020) presented a map illustrating each climate type globally at a 1 km resolution with projections for future climate types between 2071 and 2100. The Köppen climate system is globally classified into five main climate groups: Tropical, dry, temperate, continental, and polar. Besides, these groups are divided into different subgroups based on temperature (e.g., hot summer, cold summer, etc.), and seasonal precipitation (e.g., dry winter, arid desert, etc.) patterns. In total, there are thirty subgroups, which are labelled with two or three letters. The first letter corresponds to the climate group; the second letter corresponds to the precipitation pattern; and finally, the third letter is related to temperature. In this way, for example, the climate Csa corresponds to a temperate (C) hot-summer (a) Mediterranean (s) climate. Although there are thirty climate categories according to Köppen's classification (Köppen 1936), RadonPotential only includes the most common climate categories (Table 3). In any case, the developed software also allows the introduction of any other meteorological series, with local data from the region to be analyzed.

Following the methodology described by Gil-Oncina et al. (2022), the CLIGEN weather simulator (https://www.ars.usda.gov/midwest-area/west-lafayette-in/national-soil-erosion-research/docs/wepp/cligen/) has been used to generate temporal series ranging from 10 to 100 years, which include, for the selected climates, daily solar radiation, minimum and maximum temperatures, and rainfall. The input files required by CLIGEN for each climate type have been retrieved from USDA (Nicks et al. 1995). More specifically, we have selected the required input file for each climate from the longest US weather stations among all stations belonging to that climate. The CLIGEN results have been used thereafter to compute the potential evapotranspiration, ET_0, at a daily scale using a modified function of the Hargreaves equation (Williams et al 2008; Martínez et al. 2014). As part of the analysis, the first year of the time series is replicated and added to the beginning of it in order to have a training or warm-up period and get a steady and representative soil water profile for each climate type at the beginning of the simulations. After simulation, the results corresponding to this copy of the first year are discarded and not considered for further analysis. This approach mitigates the influence of subjective choices regarding the initial soil moisture content profile at the start of the simulation.

Since our objective is to evaluate the monthly average of GRP, given some specific soil and climatic conditions, the software does not accept time series shorter than 1 year, as they cannot capture the main characteristics of the specific study site.

The software: Design and implementation

The core of the program has been developed in MATLAB (2020b version) and the deployed web application has been created using MATLAB Compiler. The compiled program is executed under the MATLAB Web App Server (2020b version) application and can be run from any web browser, just invoking the following URL direction: http://www.radonpotential.com

At the beginning, the welcome window of the program is displayed (Fig. 1a). Just pressing on it, all the available options are displayed (Fig. 1b).

The main web page is structured in three main panels identified by different colors, which correspond to the input parameters associated with the soil characteristics (yellow

Table 3 Climate types selected by the RadonPotential application. The abbreviations and their corresponding definitions are obtained from the Köppen climate classification (Köppen 1936)

Abbrev	Definition	Abbrev	Definition
Af	Tropical, rainforest	Cfb	Temperate, no dry season, warm summer
Am	Tropical, monsoon	Dsa	Cold, dry summer, hot summer
Aw	Tropical, savannah	Dsb	Cold, dry summer, warm summer
Bwh	Arid, desert, hot	Dwa	Cold, dry winter, hot summer
Bwk	Arid, desert, cold	Dwb	Cold, dry winter, warm summer
Bsh	Arid, steppe, hot	Dwc	Cold, dry winter, cold summer
Bsk	Arid, steppe, cold	Dfa	Cold, no dry season, hot summer
Csa	Temperate, dry summer, hot summer	Dfb	Cold, no dry season, warm summer
Csb	Temperate, dry summer, warm summer	Dfc	Cold, no dry season, cold summer
Cfa	Temperate, no dry season, hot summer	Et	Polar, tundra

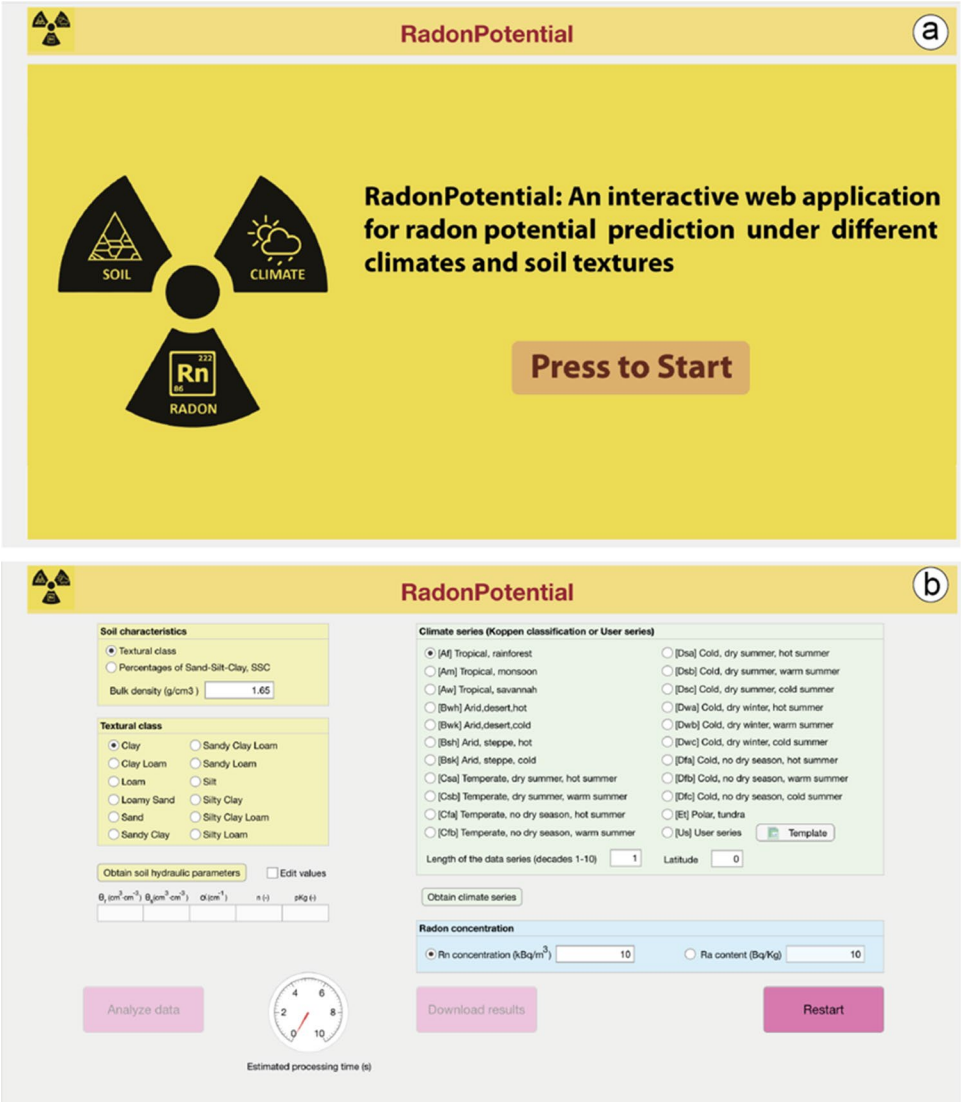

Fig. 1 Welcome window of the program (**a**) and the main web interface (**b**)

panel), the climate type (green panel), and the radon (or radium) concentrations at the site under study (blue panel).

Input parameters

The first step required by the program is the introduction of the soil characteristics by selecting the textural class (Fig. 2a, Table 2) or directly introducing the percentages of sand, silt and clay (Fig. 2b). Besides, the bulk density has also to be introduced (by default, 1.65 g cm^{-3}).

Once the properties of the soil are defined, we can obtain the soil hydraulic parameters by pressing the corresponding button.

The developed program also allows direct introduction the soil hydraulic parameters. In this case, the user has to previously activate the edit check box ('Edit values'), and once done, the soil hydraulic parameters can be introduced in their corresponding edit boxes.

The second block of input parameters (green panel) corresponds to the climate information.

The program incorporates different types of climates already predefined according to the Köppen classification (Köppen 1936). The included database allows analysis of climate series from 10 years (1 decade) to 100 years (10 decades). The length of the analyzed series is selected by the user through the corresponding edit box. Another parameter that has to be introduced by the user is the latitude of the site under study, which is used to estimate the evapotranspiration factor.

The program also allows users to introduce their climate series, by selecting the 'User series' checkbox. In this case, the format of the input file can be consulted and downloaded from the button 'Template'. In particular, the file used as a

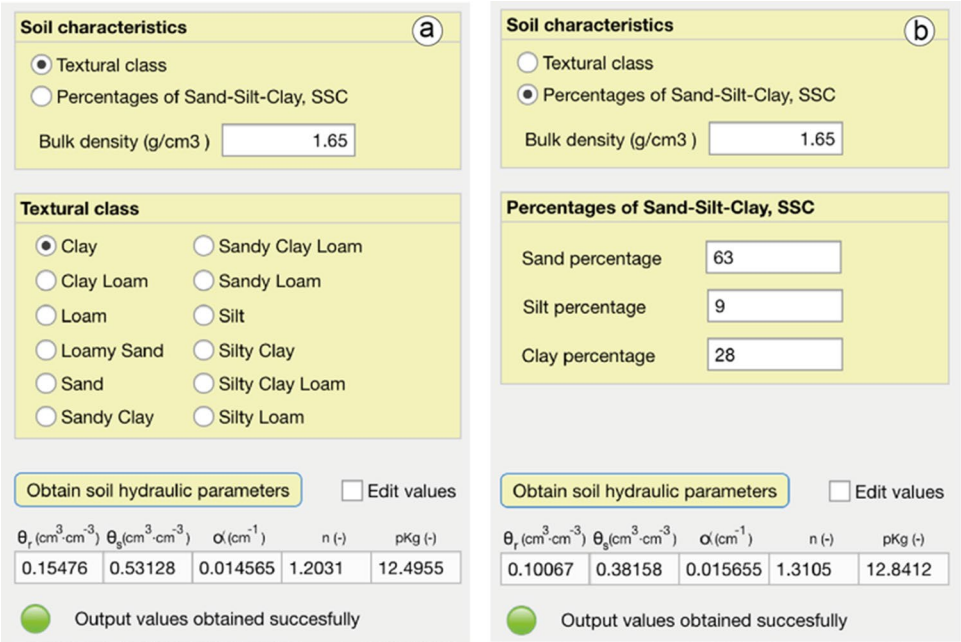

Fig. 2 Soil characteristics panel selecting 'Textural class' (**a**) or 'Percentages of Sand-Silt–Clay, SSC' (**b**)

template corresponds to the climate data series used as a case study in Sect. 4.2 (Case study 2). Figure 3 shows an example of the header and the first data columns.

The main input parameters are the precipitation and the maximum and minimum temperatures. The evapotranspiration can be included in the fourth column, but it is optional. If the input file has only three columns of data (i.e., precipitation, maximum temperature and minimum temperature), the evapotranspiration is estimated by using these parameters and the latitude.

The minimum length of the user series is 1 year. The correspondence of the climate parameters with the exact date is obtained including the initial date in the header of the file.

```
# Initial date: 01/04/2023
# Precipitation  T_max T_min Evapotranspiration (Optional)
#    (mm)         (C)   (C)         (mm)
   0.2000    8.6000    3.7000
   4.4000    9.8000    4.6000
   4.2000   11.4000    3.2000
   1.2000    9.7000    6.0000
   5.4000   12.0000    5.5000
   2.8000   14.2000    8.8000
        0   16.2000   11.1000
        0   14.0000    5.9000
   0.2000   11.9000    3.7000
   4.0000   10.7000    5.8000
  14.4000   13.5000    5.8000
        0   11.8000    8.0000
        0   11.2000    4.2000
  10.2000    8.7000    6.5000
   1.4000   10.8000    7.2000
  11.0000   14.4000    5.8000
  14.0000   10.6000    4.9000
   1.2000    9.3000    2.2000
     ...       ...       ...
```

Fig. 3 Example of the header and the first data columns of the user-defined series

Each row within the dataset corresponds to a single day. Even though the minimum accepted time length is 1 year, results from these simulations should be considered with caution because the monthly average results are computed based on only 1 month.

Once selected the climate input options, the climate series can be retrieved by pressing the corresponding button. The program checks the selected series (especially in the case of a user series) and prepares the data for the subsequent analysis.

Finally, depending on the available information, the user can enter the mean measured radon or radium concentration in the last input parameter block (blue panel).

Data analysis

By default, the analysis of the data is not available since all the input parameters have been checked and everything is correct. If they are right, then the 'Analyze data' button will be activated, ready to run the analysis.

The core of the analysis is based on the HYDRUS-1D software (Šimůnek et al. 2009), which is called from the web application and executed as a command line. HYDRUS-1D extracts the required soil and climate characteristics from some input files, which are prepared by the developed program for each specific case and user.

Once any user enters the web page, a temporal folder is created for executing HYDRUS-1D and all the required files are saved. Besides, the input data and the output results are also saved in this temporal folder. After five hours, this temporal folder is removed. In this way, the web application

can be run by several users at the same time without any problem.

The input files required by HYDRUS-1D are: PROFILE.DAT, HYDRUS1D.DAT, ATMOSPH.IN and SELECTOR.IN.

Before starting, the program calculates a rough estimation of the processing time in order to show the user a clock with the progress of the analysis.

When convergence problems appear, the software indicates to the user that the run has failed. Convergence problems may appear for different reasons: (1) coarse soil discretization, (2) abrupt changes in atmospheric conditions, and/or (3) in the soil water retention curves (as it usually happens with sandy soils). The RadonPotential software takes care of the numerical soil discretization and lets the user take care of the others.

Output results

The results of the calculation are provided by HYDRUS-1D through the output file Obs_Node.out, which is saved in the corresponding temporal folder. According to this output file, RadonPotential returns a graphical output with the following results:

1) Average value of the maximum and minimum temperatures of each month of the year.
2) Average value of the precipitations and evapotranspiration of each month of the year.
3) Average volumetric water content at different depths of soil (20, 50, 80 and 100 cm) for each month of the year. The histogram and some statistical parameters of the volumetric water content at 1 m depth are also shown.
4) Average permeability at different depths of soil (20, 50, 80 and 100 cm) for each month of the year. The histogram and some statistical parameters of the permeability at 1 m depth are also shown.
5) Average Geogenic Radon Potential for each month of the year. The histogram and some statistical parameters of the GRP are also shown. Besides, a traffic light criterium is used to classify the radon potential in low (GRP < 10), medium (10 ≤ GPR < 35), and high (GRP ≥ 35) risks.

Each of these graphs can be downloaded in.jpeg format by the user.

Moreover, once the calculations have been completed, the 'Download result' button is enabled, allowing users to download the obtained results in a compressed zip file, 'results.zip'. This file includes two ASCII files, 'results_daily.txt' and 'results_monthly.txt', which provide the results obtained for every day of the analyzed period, and the average results obtained for every month of the year, respectively. In both cases, they provide the following information: maximum and minimum temperatures, precipitation, evapotranspiration, volumetric water content, permeability, and GRP (Fig. 4).

Application and results

In this section, two case studies have been selected to examine the estimation of radon potential under different climate scenarios. The first case study focuses on a 100-year climate series in the Cfb climate type, whereas the second case study evaluates a one-year local weather time series in an area prone to radon. Each case presents two approaches for assessing radon concentration. The first scenario involves using a constant radon concentration, typically obtained from onsite field measurements, which serves as a representative value for the area. In contrast, the second scenario estimates radon concentration from ^{226}Ra activity (Eq. (5)). This calculation considers factors such as soil texture, water content, and temperature, resulting in variations in radon activity. Radon concentration in soil temporally varies due to soil response to climatic factors and soil conditions. Soil water content is the parameter likely to exert the most significant influence on radon in soil air. However, its response to rainfall events and variability within the soil depth depends on the type of soil. Barometric pressure, temperature, and wind also affect radon soil activity, although their impact is less significant (Voltaggio 2012; Cinelli et al 2019). Consequently, radon dynamics in the soil may be more accurately represented considering the second approach rather than a constant value because it includes the variation of radon concentration and gas permeability due to changes in soil textures and properties (hydraulic properties, water content, temperature, density, etc.).

Case study 1

In this case study, we have selected a 100-year climate series (10 decades), representing a Cfb climate type commonly observed in western Europe and North America (Beck et al. 2020). Cfb climates have mild summers and cool to mild winters and receive a moderate to high amount of precipitation throughout the year. Rainfall is evenly distributed, with no distinct dry season. The soil type selected for this study is loam ($\rho_b = 1.57$ g cm−3), which is prevalent, for example, across Europe as indicated by the LUCAS database (Ballabio et al. 2016). The specific radon concentration chosen as an example for analysis is a median value of 67 kBq m−3 (Friske et al. 2014). This value can

Fig. 4 Example of results files: 'results_daily.txt' (**a**), and 'results_monthly.txt' (**b**)

(a)

```
Day Tmax Tmin Precipitation Evapotranspiration Volumetric_Water_Content pKg GRP
# C C mm mm (-) (-) (-)
1 3.8 -5.7 34.3 1.7658 0.34674 19.756 6.8675
2 6.6 -0.2 5.9 1.8623 0.35898 20.596 6.3232
3 5.6 -2 15.9 1.8374 0.38262 23.286 5.0428
4 4.4 -1.2 0.3 1.5611 0.36556 21.153 6.0073
5 2.3 -5.6 15.5 1.5433 0.35448 20.262 6.5291
6 7.1 2 24.5 1.7166 0.34957 19.932 6.7457
7 11.1 4.1 0 2.2858 0.34137 19.445 7.0938
8 6 3 0 1.3136 0.3337 19.046 7.407
9 8.1 1.3 0 1.9954 0.31912 18.396 7.98
10 12.8 8.4 5.3 2.0264 0.32471 18.63 7.7634
```

(b)

```
Month Tmax Tmin Precipitation Evapotranspiration Volumetric_Water_Content pKg GRP
# C C mm mm (-) (-) (-)
1 6.0223 0.040097 520.38 51.986 0.34802 19.835 6.8127
2 8.5478 0.80914 388.22 61.544 0.34011 19.376 7.1457
3 10.432 1.0122 374.7 79.568 0.33686 19.204 7.2793
4 13.278 2.5007 239.16 86.947 0.31254 18.139 8.2322
5 16.945 4.97 131.02 100.22 0.28902 17.35 9.1158
6 19.83 7.9317 83.761 101.97 0.26022 16.573 10.193
7 22.443 9.4117 54.69 119.28 0.26259 16.631 10.103
8 22.628 9.8423 64.022 126.19 0.24413 16.2 10.806
9 20.086 7.9606 145.11 115.89 0.22979 15.894 11.368
10 14.864 4.8142 309.77 95.478 0.25517 16.452 10.384
11 9.2933 2.3514 467.51 62.657 0.33639 19.18 7.2982
12 6.2825 0.68235 522.33 51.24 0.3445 19.623 6.9626
```

be considered as average, given that radon concentration exhibits strong temporal variability due to climatic fluctuations. The influence of climatic parameters on radon concentration will be analyzed in Case Study 2, where radon concentration is estimated with a constant radium concentration and variable water saturation and temperature. Case Study 1, therefore, serves as a clear example to evaluate the influence of climatic parameters on the Geogenic Radon Potential risk at a local scale. Figure 5 exhibits the selected parameters within the input windows.

In Fig. 6, the meteorological characteristics of the Cfb climate are summarized, along with the volumetric water content calculated at various depths ranging from 20 to 100 cm. The volumetric water content is observed to be lower near the surface compared to deeper depths (100 cm) due to the influence of evapotranspiration (ET0) on the surface soil. As the volumetric water content increases, the soil becomes less permeable, indicated by higher pkg values. The existence of liquid water in the soil's porosity reduces pore section and porosity, thereby affecting gas transport. Consequently, the variation in water content describes the permeability pattern. Additionally, the results highlight the sensitivity of permeability to soil depth and, especially, to seasonal changes. Thus, during humid months, the soil exhibits higher water content and, consequently, higher pkg values. Conversely, during dry months, the soil becomes more permeable as water content decreases due to reduced precipitation and intensive evapotranspiration.

The variation in permeability directly impacts the GRP, transitioning from lower radon potential during wet periods to medium radon potential in dry months. In this particular case study, the radon concentration remains constant throughout the calculations, considering, for example, a representative value for a specific soil type or lithology. The study does not evaluate the significant fluctuations in radon caused by climatic parameters in the GRP estimation. Such influences could be analyzed by defining a range, distribution, or percentage of radon concentration values that encompass these effects.

Case study 2

This case study focuses on a one-year local climatic series in a radon-prone area. The evaluated soils are derived from granite alteration, which contains uranium and radium, leading to notable concentrations of radon gas.

The studied soils are part of the Alpedrete formation, situated in the Guadarrama Mountains of the Central System (Spain). According to the predictive radon exposure map of the National Safety Council (2017), the area belongs to the medium–high radon exposure category. In terms of soil classification, these soils can be identified as loamy sand, characterized by a composition of sand (74%), silt (24%), and clay (2%). The bulk density of the soil measures 1.68 g cm−3. Additionally, the activity of 226Ra is recorded at 39.7 Bq Kg−1. The climate series parameters have been

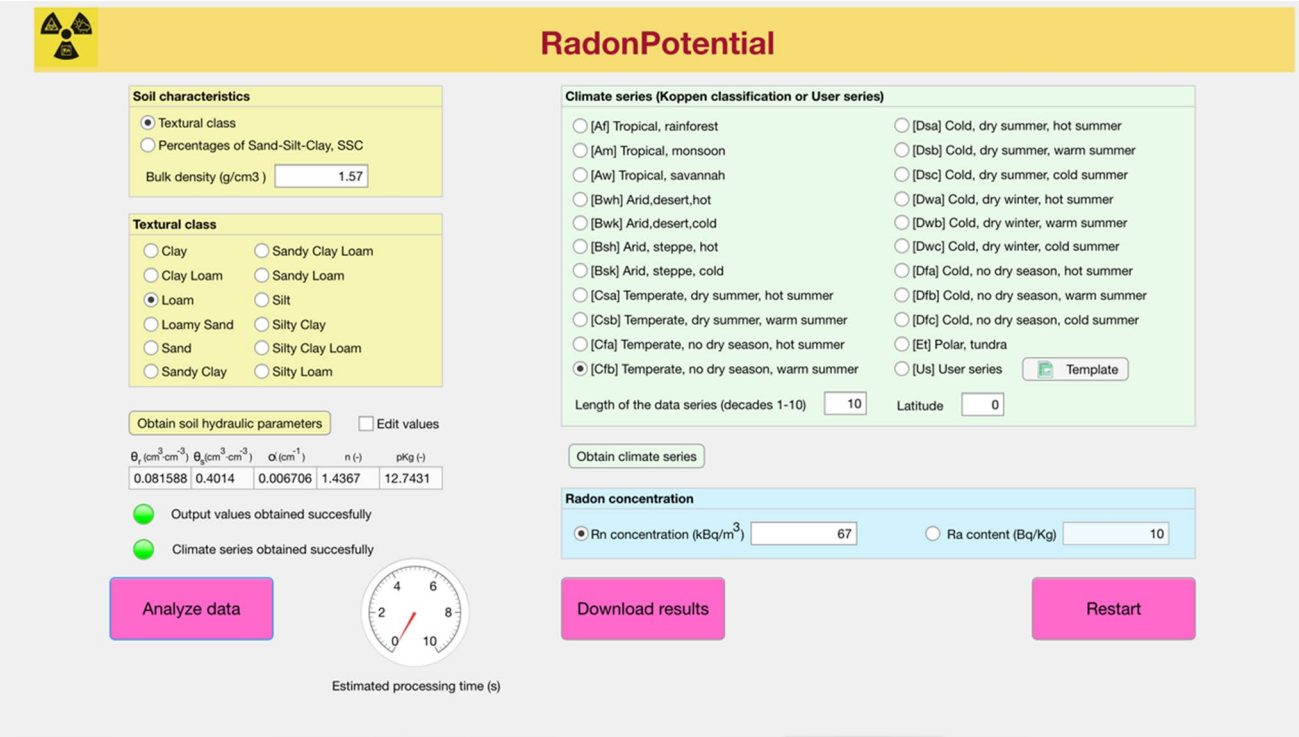

Fig. 5 Parameters selected for Case study 1

derived from the Alpedrete climatic station's data for the year 2021 (Agencia Estatal de Meteorología, AEMET. Registros climáticos El Boalo, 2021) (https://opendata.aemet.es/centrodedescargas/productosAEMET). According to the Köppen-Geiger climate classification, the climate in this region can be categorized as Csa-Csb.

Figure 7 shows the selected parameters within the different panels. In contrast to the previous case study, this analysis incorporates a specific soil texture determined by the percentage of sand, silt, and clay (% SSC), as well as the bulk density. Additionally, a one-year local weather time series and the radium activity data are employed in this study. This climate data series can be downloaded through the Template button.

Figure 8 exhibits the climatic parameters recorded throughout the year 2021. Volumetric water content is displayed at various depths ranging from 20 to 100 cm, demonstrating a fluctuating pattern closely linked to evapotranspiration and irregular rainfall. For instance, despite similar precipitation levels in October, there were notable differences in evapotranspiration (ET0). The months with the highest rainfall were February, April, and September, resulting in higher water content in the soil, even near the surface, compared to deeper depths. Gas permeability follows a similar trend, with August being the month characterized by the highest permeability in the soil, aligning with elevated temperatures and ET0. However, permeability decreases after the September rains. Additionally, the results reveal substantial permeability variations primarily in shallower depths. The fluctuation in permeability, along with the concentration of 222Rn derived from the initial 226Ra, directly influences the GRP, which tends to be higher during drier months.

RadonPotential emphasizes the significance of considering not only soil texture and climatic conditions but also water content, radon concentration, and permeability depth measurements when assessing GRP. Changes in the classification of GRP become more critical when incorporating alternative classifications, such as the one proposed by Elío et al. (2020), which includes categories such as low ($GRP < 10$), low-moderate ($10 \leq GRP < 22.5$), moderate-high ($22.5 \leq GRP < 30$), and high ($GRP \geq 30$) risk.

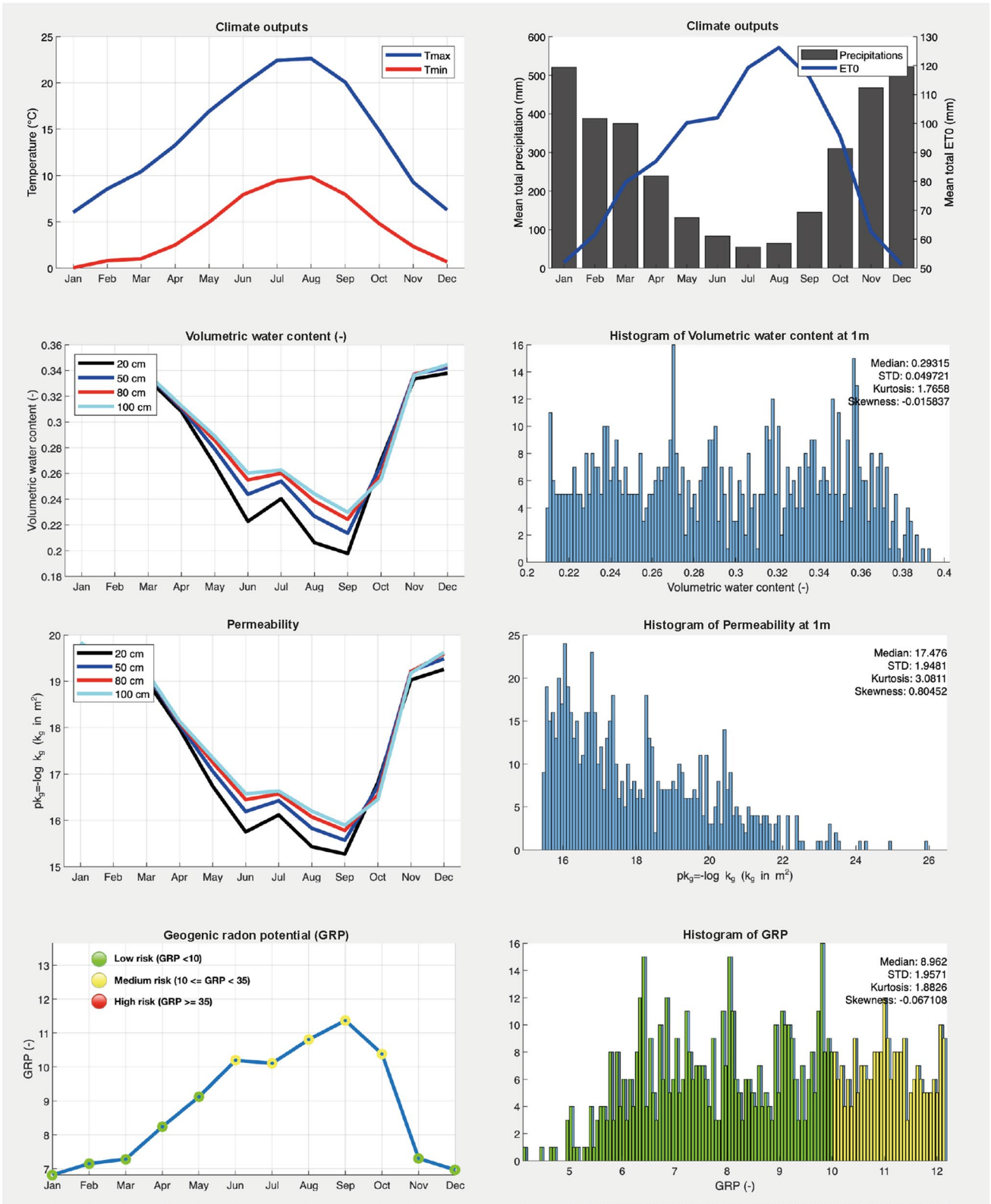

Fig. 6 Graphical results obtained for Case study 1

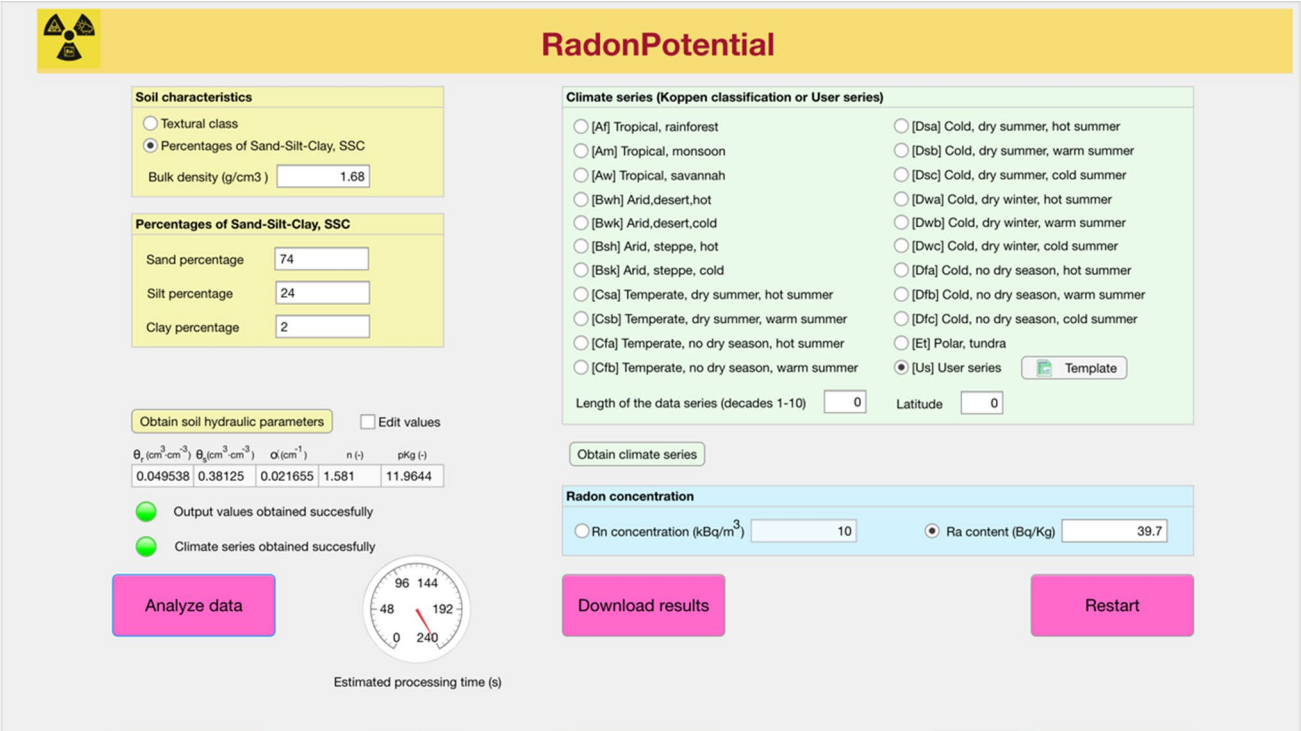

Fig. 7 Parameters selected for Case study 2

Conclusions

In this work, a new theoretical scheme is proposed to estimate the geogenic radon potential by taking into account climate and soil texture variations. Using the appropriate equations, radon concentration and permeability through soil profiles are calculated based on soil texture and water content. We also consider the dynamics of soil water content across different climates, incorporating long-term weather data from various climatic scenarios as well as local weather time series.

The proposed procedure has been implemented under a novel web-based software tool, RadonPotential, which emphasizes the importance of considering radon and gas permeability all together with soil texture and climatic conditions to obtain an accurate radon potential assessment.

Two case studies have been selected to assess the estimation of radon potential in different climate scenarios. The first case study focuses on a 100-year climate series in the Cfb climate type commonly observed in Western Europe and North America. The second case study evaluates a one-year local weather time series in an area prone to radon.

Thus, the conceived methodology provides valuable insights for the development of more reliable large-scale radon risk maps, that account for spatial variability in geochemical and textural soil characteristics, as well as temporal variability related to climatic factors.

The web-based format of the implemented program enhances its accessibility, usability, and manageability to a wider user base compared to any other program that requires installation on a computer. Therefore, the RadonPotential program serves as a valuable tool for scientists, technical experts, and policymakers in developing strategies for measurement, mitigation, and action related to radon in both existing and newly constructed buildings.

Once the main objectives of the present work have been carried out, an exhaustive quantitative and statistical uncertainty analysis will be the object of future research works.

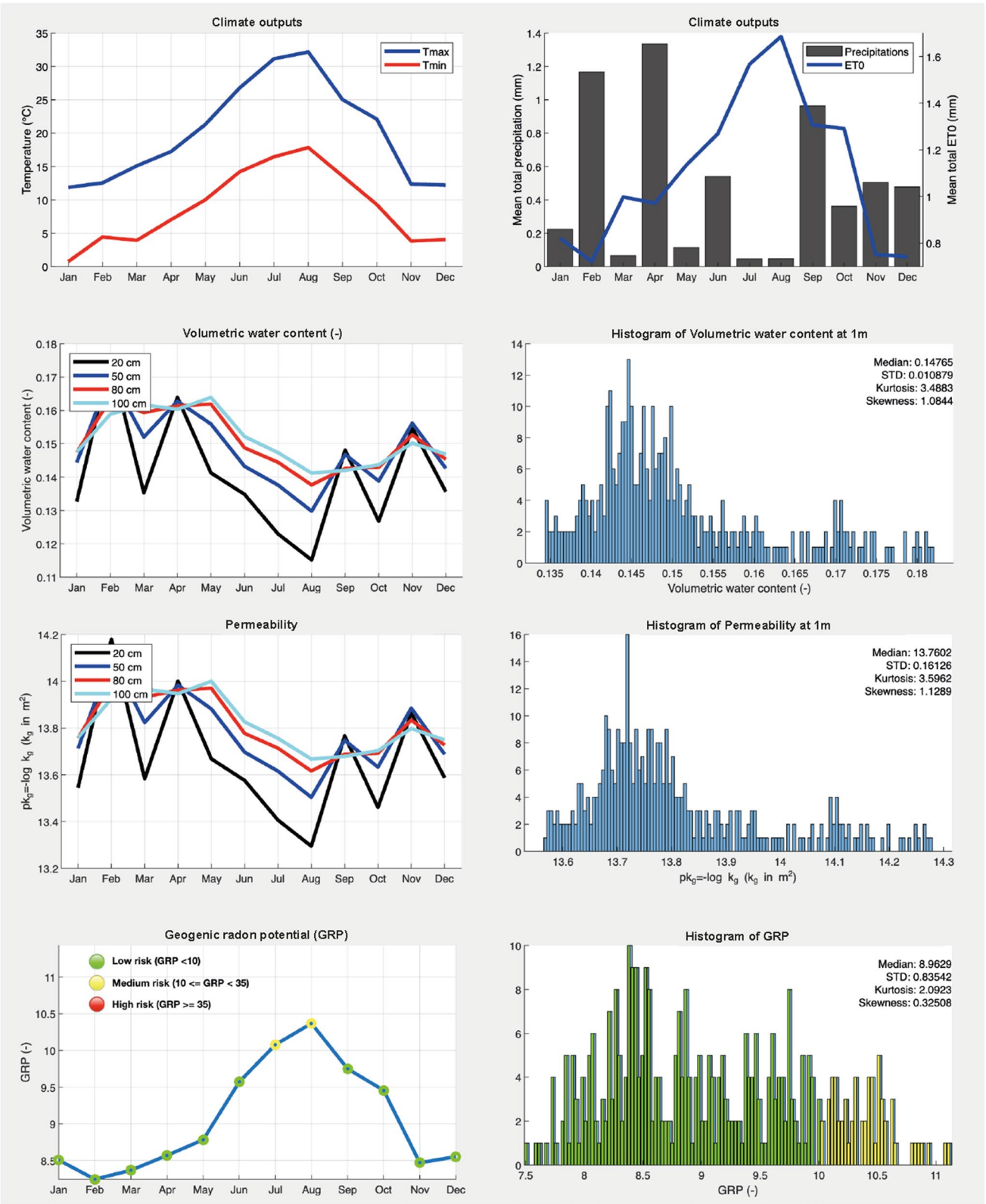

Fig. 8 Graphical results obtained for Case study 2

Availability and Requirements

RadonPotential is a web application, therefore no installation process is necessary. It can be accessed at the website http://www.radonpotential.com (without registration, free of charge) from any browser such as Chrome, Edge, Safari or Firefox installed on a computer. Matlab App Server does not allow running on mobile phones.

Acknowledgements We thank the support of the research group VIGROB-116 (University of Alicante). A pre-doctoral research fellowship (PRE2019-088294) was awarded to S. Gil-Oncina for the project RTI2018-099052-BI00. The authors wish to thank Geomnia for their sample provision and data support of the Alpedrete site.

Author's contributions David Benavente and Javier Valdes-Abellan contributed to the conception and design of the work. Juan Jose Galiana-Merino, Juan Luis Soler-Llorens and Javier Valdes-Abellan programmed the software. Juan Jose Galiana-Merino, Sara Gil-Oncina and Juan Luis Soler-Llorens tested the software. David Benavente, Sara Gil-Oncina and Javier Valdes-Abellan contributed to the analysis and interpretation of data. Juan Jose Galiana-Merino, Sara Gil-Oncina, Javier Valdes-Abellan and David Benavente wrote the main manuscript text and prepared figures. All authors reviewed the manuscript.

Funding Open Access funding provided thanks to the CRUE-CSIC agreement with Springer Nature. This work has been partially supported by the Spanish Government (grant numbers RTI2018-099052-B-I00 and PID2021-123135OB-C21), and by the Conselleria de Innovación, Universidades, Ciencia y Sociedad Digital de la Generalitat Valenciana (project CIAICO/2022/038).

Data availability The climate database, predefined according to the Köppen classification (Köppen 1936), as well as the data used for the Case study 2 are available at the link https://github.com/JLSolerLlorens/RadonPotential.

Code availability The source code and all the required files are available for download at the link https://github.com/JLSolerLlorens/RadonPotential.

Declarations

Competing interests The authors declare no competing interests.

Consent for publication If the article is accepted by the Editor-in-chief after the review process, all authors consent to the manuscript being published in Earth Science Informatics. The work did not include human participants in order to obtain their consent.

References

Akerblom G (1993) Ground radon: Monitoring procedure in Sweden. In: Lecture at the "JAG" Disc. Meeting on" Radon Workshop, Geology, Environment, Technology". Royal Astr. Soc.

Alegría N, Hernández-Ceballos MÁ, Cinelli G, Peñalva I, Muñoz JM (2023) Analysis of 222Rn Surface Concentrations in the Basque Country (Spain): A Case Study of Heat Waves. Int J Environ Res Public Health 20(3):2105. https://doi.org/10.3390/ijerph20032105

Appleton JD (2007) Radon: sources, health risks, and hazard mapping. Ambio 36(1):85–89

Ballabio C, Panagos P, Montanarella L (2016) Mapping topsoil physical properties at European scale using the LUCAS database. Geoderma 261:110–123. https://doi.org/10.1016/j.geoderma.2015.07.006

Beck HE, Zimmermann NE, McVicar TR, Vergopolan N, Berg A, Wood EF (2020) Publisher Correction: Present and future Köppen-Geiger climate classification maps at 1-km resolution. Sci Data 7:274. https://doi.org/10.1038/s41597-020-00616-w

Benavente D, Pla C (2018) Effect of pore structure and moisture content on gas diffusion and permeability in porous building stones. Mater Struct 51(1):21. https://doi.org/10.1617/s11527-018-1153-8

Benavente D, Valdés-Abellán J, Pla C, Sanz-Rubio E (2019) Estimation of soil gas permeability for assessing radon risk using Rosetta pedotransfer function based on soil texture and water content. J Environ Radioact 208:105992. https://doi.org/10.1016/j.jenvrad.2019.105992

Bossew P, Cinelli G, Ciotoli G, Crowley QG, De Cort M, Elío J, Gruber V, Petermann E, Tollefsen T (2020) Development of a geogenic radon hazard index—concept, history, experiences. Int J Environ Res Public Health 17(11):4134. https://doi.org/10.3390/ijerph1711413

Cinelli G, Tollefsen T, Bossew P, Gruber V, Bogucarskis K, De Felice L, De Cort M (2019) Digital version of the European Atlas of natural radiation. J. Environ. Radioact. 196:240–252. https://doi.org/10.1016/j.jenvrad.2018.02.008

de Farias EEG, da Silva Neto PC, de Souza EM et al (2016) Radon levels and transport parameters in Atlantic Forest soils. J Radioanal Nucl Chem 307:811–815. https://doi.org/10.1007/s10967-015-4268-1

Demetriades A, Reimann C, Birke M, Négrel P, Ladenberger A, Tarvainen T, Sadeghi M, the GEMAS Project team (2021) GEMAS: Geochemistry of European agricultural and grazing land soil. Eur Geol 52:21–32. https://zenodo.org/records/5770107

Elío J, Crowley Q, Scanlon R, Hodgson J, Zgaga L (2018) Estimation of residential radon exposure and definition of Radon Priority Areas based on expected lung cancer incidence. Environ Int 114:69–76. https://doi.org/10.1016/j.envint.2018.02.025

Elío J, Cinelli G, Bossew P, Gutiérrez-Villanueva JL, Tollefsen T, De Cort M, Nogarotto A, Braga R (2019) The first version of the pan-European indoor radon map. Nat Hazards Earth Syst Sci 19(11):2451–2464. https://doi.org/10.5194/nhess-19-2451-2019

Elío J, Crowley Q, Scanlon R, Hodgson J, Long S, Cooper M, Gallagher V (2020) Application of airborne radiometric surveys for large-scale geogenic radon potential classification. Journal of the European Radon Association 17:1. https://doi.org/10.35815/radon.v1.4358

Friske PWB, Ford KL, McNeil RJ, Pronk AG, Parkhill MA, Goodwin TA (2014) Soil geochemical, mineralogical, radon and gamma ray spectrometric data from the 2007 North American soil geochemical landscapes project in New Brunswick, Nova Scotia and Prince Edward Island. rev., Geological Survey of Canada, Open File, 6433. https://doi.org/10.4095/293020

Galiana-Merino JJ, Molina S, Kharazian A, Toader VE, Moldovan IA, Gómez I (2022) Analysis of Radon Measurements in Relation to Daily Seismic Activity Rates in the Vrancea Region. Romania Sensors 22(11):4160. https://doi.org/10.3390/s22114160

Gil-Oncina S, Valdes-Abellan J, Pla C, Benavente D (2022) Estimation of the Radon Risk Under Different European Climates and Soil Textures. Front Public Health 10:794557. https://doi.org/10.3389/fpubh.2022.794557

Giustini F, Ciotoli G, Rinaldini A, Ruggiero L, Voltaggio M (2019) Mapping the geogenic radon potential and radon risk by using Empirical Bayesian Kriging regression: A case study from a volcanic area of central Italy. Sci Total Environ 661:449–464. https://doi.org/10.1016/j.scitotenv.2019.01.146

Gruber V, Bossew P, De Cort M, Tollefsen T (2013) The European map of the geogenic radon potential. Journal of Radiological Protection: Official Journal of the Society for Radiological Protection 33:51–60. https://doi.org/10.1088/0952-4746/33/1/51

Köppen W (1936) Das geographische System der Klimate. In: Handbuch der Klimatologie, band I, teil C, 46. Edited by Köppen, W. and Geiger. Berlin

Martínez G, Pachepsky YA, Vereecken H (2014) Temporal stability of soil water content as affected by climate and soil hydraulic properties: A simulation study. Hydrol Process 28(4):1899–1915. https://doi.org/10.1002/hyp.9737

Morales-Simfors N, Wyss RA, Bundschuh J (2020) Recent progress in radon-based monitoring as seismic and volcanic precursor: A critical review. Crit Rev Environ Sci Technol 50(10):979–1012. https://doi.org/10.1080/10643389.2019.1642833

Mualem Y (1976) A new model for predicting the hydraulic conductivity of unsaturated porous media. Water Resour Res 12(3):513–522. https://doi.org/10.1029/WR012i003p00513

Neznal M, Neznal M, Matolín M, Barnet I, Miksova J (2004) The new method for assessing the radon risk of building sites. Prague: Czech Geological Survey, p 48

Nicks AD, Lane LJ, Gander GA (1995) Weather generator. In: West Flanagan DC, Nearing MA (eds) USDA-Water erosion prediction project: Hillslope profile and watershed model documentation

Petermann E, Meyer H, Nussbaum M, Bossew P (2021) Mapping the geogenic radon potential for Germany by machine learning. Sci Total Environ 754:142291. https://doi.org/10.1016/j.scitotenv.2020.142291

Pla C, Ruiz MC, Gil-Oncina S, García-Martínez N, Cañaveras JC, Cuezva S, Fernández-Cortés Á, Sánchez-Moral S, Benavente D (2023) 222Rn and CO2 monitoring in soil and indoor atmosphere to understand changes in the gaseous dynamics of Rull cave (Spain). Environ Earth Sci 82(9):235. https://doi.org/10.1007/s12665-023-10885-4

Richards LA (1931) Capillary conduction of liquids through porous mediums. J. Applied Physics 1:318–333. https://doi.org/10.1063/1.1745010

Šimůnek J, Šejna M, Saito H, Sakai M, van Genuchten MT (2009) The HYDRUS-1D package for simulating the movement of water, heat, and multiple solutes in variably saturated media, version 4.08. Department of Environmental Sciences, University of California, Riverside, California, USA

Tareen ADK, Nadeem MSA, Kearfott KJ, Abbas K, Khawaja MA, Rafique M (2019) Descriptive analysis and earthquake prediction using boxplot interpretation of soil radon time series data. Appl Radiat Isot 154:108861. https://doi.org/10.1016/j.apradiso.2019.108861

USDA, United States Department of Agriculture (1987) Soil mechanics level 1, Module 3. USDA Textural Classification Study Guide

Van Genuchten MTh (1980) A closed form equation for predicting the hydraulic conductivity of unsaturated soils. Soil Sci Soc Am J 44:892–898. https://doi.org/10.2136/sssaj1980.03615995004400050002x

Victor NJ, Siingh D, Singh RP, Singh R, Kamra AK (2019) Diurnal and seasonal variations of radon (222Rn) and their dependence on soil moisture and vertical stability of the lower atmosphere at Pune. India Atmos Sol Terr Phys 195:105118. https://doi.org/10.1016/j.jastp.2019.105118

Vital M, Grondona S, Dimova N, Martinez DE (2022) Factors affecting the radon (222Rn) emanation from aquifer rock materials: Implications for radiological and groundwater tracer studies. Appl Radiat Isotopes 189:110433. https://doi.org/10.1016/j.apradiso.2022.110433

Voltaggio M (2012) Radon progeny in hydrometeors at the earth's surface. Radiat Prot Dosimetry 150:334–341

Voltaggio M, Masi U, Spadoni M, Zampetti G (2006) A methodology for assessing the maximum expected radon flux from soils in northern Latium (central Italy). Environ Geochem Health 28:541–551. https://doi.org/10.1007/s10653-006-9051-3

Williams JR, Izaurralde RC, Steglich EM (2008) Agricultural policy/environmental extender model. Theoretical Documentation, Version, 604, pp 2008–2017

World Health Organization (2009) WHO Handbook on Indoor Radon: A Public Health Perspective; World Health Organization: Geneva, Switzerland, p 94

Zhang Y, Schaap MG (2017) Weighted recalibration of the Rosetta pedotransfer model with improved estimates of hydraulic parameter distributions and summary statistics (Rosetta3). J Hydrol 547:39–53. https://doi.org/10.1016/j.jhydrol.2017.01.004

Zhuo W, Iida T, Furukawa M (2006) Modeling radon flux density from the earth's surface. J Nucl Sci Technol 43(4):479–482. https://doi.org/10.3327/jnst.43.479

Zhuo W, Guo Q, Chen B, Cheng G (2008) Estimating the amount and distribution of radon flux density from the soil surface in China. J Environ Radioact 99(7):1143–1148. https://doi.org/10.1016/j.jenvrad.2008.01.011